Nonlinear dynamics control in single-phase inverter with sinusoidal pulse-width modulation

A I Andriyanov and D Yu Mikhal'tsov
Department of Electronics, Radioelectronic and Electrotechnical Systems, Bryansk State Technical University, 7, 50 years of October st., Bryansk, 241035, Russia

E-mail: mail@ahaos.ru

Abstract. A variant of technical implementation of the control system of a single-phase voltage inverter with sinusoidal pulse-width modulation, based on target-oriented control, which ensures the desired nonlinear dynamic properties of the system, is proposed. The control system under discussion solves the problem of providing a sinusoidal output voltage of the inverter when changing its parameters in a wide range, accompanied by bifurcations. This eliminates unwanted dynamic modes without parametric synthesis of the system. The target-oriented control for managing the dynamics of nonlinear systems with sinusoidal pulse-width modulation is used for the first time and gives a number of advantages compared to other known methods.

1. Introduction

Today, single-phase bridge inverters with sinusoidal pulse-width modulation (SPWM) are widely used in machine engineering that require DC/AC conversion. Such systems include uninterruptible power supplies, passenger car power supply systems, AC welding equipment, variable speed control, induction heats, etc. [1]. The equipment discussed is provided with control loops with voltage feedback that usually have complex dynamics [2, 3]. As a result of bifurcations, when changing settings in such systems, one may experience unwanted dynamic modes, accompanied by a significant harmonic distortion of the output voltage, which causes the spread of noise to the load, current overload of the power switches, or acoustic effects during operation. To prevent such consequences, specific nonlinear dynamics control algorithms are required.

There are many reports on the control of nonlinear dynamics of discrete systems [4-9]. Two key types of control can be mentioned: linearization of the Poincare map [4] and time-delay feedback control methods [5, 6]. There is also a well-known approach based on a so-called resonant perturbation of parameters [7]. The application of above methods in power electronics has been widely reported in the scientific literature. Most of the reports are dedicated to the control of nonlinear dynamics of DC/DC converters, while SPWM converters are mentioned in a fewer number of articles [8-9]. In [8], the possibility of using a resonant perturbation of parameters in the SPWM system in order to stabilize the design dynamic mode is discussed. Here, the control action perturbation was specified as a harmonic signal. In the same report, the possibility of applying a time-delay feedback control was discussed. The application of slope compensation method, which is a version of the resonant perturbation of parameters, was discussed in [9], where the perturbation was specified as a linearly falling signal. The disadvantages of the reports include the lack of analysis of efficiency of the methods discussed when the system parameters are changed over a wide range. For example, the

following parameters may vary during an actual voltage converter operation: load impedance, input voltage, or a reference signal, which causes complex dynamic modes, even when the mentioned algorithms are used. When changing system parameters, the control method parameters shall be adapted, that stipulates high demands to microcontroller resources. The linearization of the Poincare map has never been applied to SPWM systems due to the very high demands to computing resources required to calculate the corrective actions.

In [10] the so-called target-oriented control (TOC) is discussed, which allows expanding the possibilities of the design mode stabilization over a wide range of system parameters variation compared to the above mentioned methods. In [11], the possibility of using this method to control the nonlinear dynamics of a DC/DC converter is discussed, where the method has proved its efficiency.

The main objective of this report is creation of the TOC-based control system of a SPWM single-phase voltage inverter, with minimum microcontroller speed requirements, which provides the design dynamic mode over a predetermined range of system parameters variation.

For the purpose of this report, the design dynamic mode means a mode where the process period is the same as the reference sinusoidal signal period. This mode is called 1-cycle [2]. Wherein, the SPWM duty cycle over all cycle periods within the control signal period is: $0<\gamma<1$. Unwanted *m*-cycles are also possible, where the period of processes in the system is *m* times longer than that of the reference sinusoidal signal. Hereinafter, *m* indicator is called a cycle factor.

2. Target-oriented control of nonlinear dynamics

Suppose there is a discrete system described by a function of the stroboscopic map:

$$x_n = f(x_{n-1}), \tag{1}$$

where x_n - variable value in the n^{th} iteration of the map.

According to [10], the unstable fixed point map (1) x^* can be stabilized by adding a stabilizing effect, where the stroboscopic map for the nonlinear dynamic system is as follows:

$$x_n = f(x_{n-1}) + c(x^* - f(x_{n-1})), \tag{2}$$

where *c* - adjustable factor. According to (2), when the system is in the steady mode, the second term vanishes.

The main problem of this method is the need to precalculate the stabilized fixed point, which, in case of higher order maps, is complicated and involves high computational cost.

3. Single-phase voltage inverter control system

The functional diagram of the SPWM single-phase voltage inverter of the TOC-based control system is shown in Figure 1.

Following designations are used here: *R* - inductor resistance; *L* - inductor inductance; *C* - capacitor capacitance, R_L - load resistance, *VT*1-*VT*4 - power switches; *VD*1-*VD*4 - power diodes; U_{in} - input voltage; α - proportional controller gain; β, β_1, β_2 - feedback loop gains; U_{ref} - reference signal; U_p - power switch control pulses; U_{con} - control signal; U_r - ramp signal; *MCS* - main control system; *ACS* - auxiliary control system; *MC* - master clock; *RG* - ramp generator; *C* – comparator; *SH*, *SH*1, *SH*2 - sample & hold circuits; *NOT* – NOT-gate; *FPC*1 and *FPC2* - fixed point maps computer; *SB*1 and *SB*2 - subtracters; *LRC* - load resistance computer; K_1, K_2 - gains; U_{err} - *MCS* error; x_{1kref}, x_{2kref} - components of 1-cycle fixed point vector; x_{1clk}, x_{2clk} - components of the feedback vector in terms of state variables in stroboscopic time points; u_{1k}, u_{2k}, - components of the control actions vector.

The control system (*CS*) shown in Figure 1 can be divided into two subsystems. The main control subsystem provides stabilization of the average value of the output voltage without regard to nonlinear dynamic properties. The auxiliary control subsystem provides the desired stabilization of the design dynamic mode (1-cycle).

Figure 2 shows signal waveforms when using SPWM of the first kind, applied in microprocessor-based control systems [2]. Designations in Figure 2 correspond to those in Figure 1.

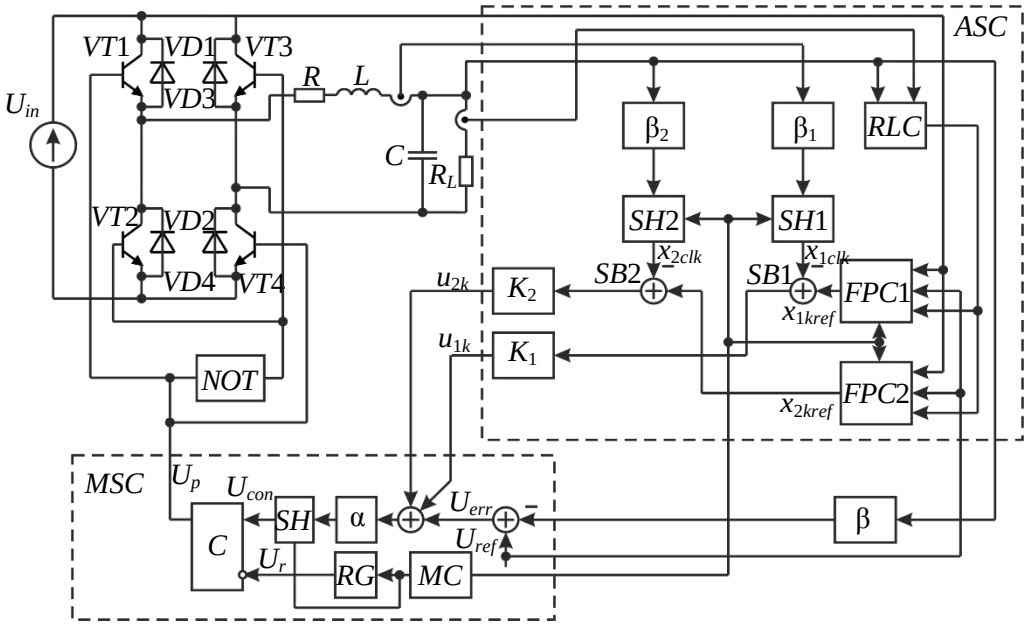

Figure 1. SPWM voltage converter control system

The cycle period is divided into two segments of structure constancy of the power unit (Fig. 2):

1) Segment 1: $0<z<z_k$. In this segment, the power switches, *VT*1 and *VT*4, are closed and positive voltage (U_{fin} in Fig. 2) is supplied to the filter input;

2) Segment 2: $z_k<z<1$. In this segment, the power switches, *VT*2 and *VT*3, are closed and negative voltage is supplied to the filter input.

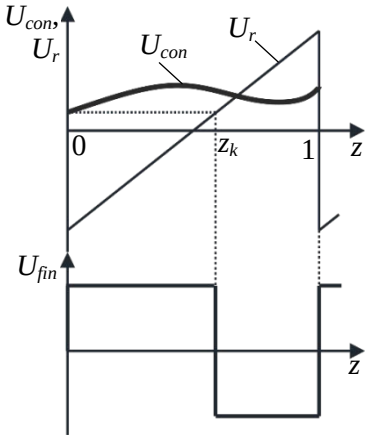

Figure 2. SPWM voltage converter waveforms

The point of switching in the relative time in the k^{th} cycle period is calculated as

$$z_k = \frac{t_k - (k-1)T}{T},$$

where t_k - point of switching in absolute time, T - modulation period, k - number of the cycle period.

At each segment of structure constancy of the power unit, the movements are described by a linear differential equations system that has the following matrix form:

$$\frac{d\mathbf{X}}{dt} = \mathbf{A}_i\mathbf{X} + \mathbf{B}_i, \tag{3}$$

where $\mathbf{A}_i$ - matrix of constant factors in the i^{th} segment, $\mathbf{B}_i$ - forcing vector in the i^{th} segment, i = 1, 2, $\mathbf{A}_1 = \begin{bmatrix} -\frac{R}{L} & -\frac{1}{L} \\ \frac{1}{C} & -\frac{1}{CR_L} \end{bmatrix}$, $\mathbf{B}_1 = \begin{bmatrix} U_{in}/L \\ 0 \end{bmatrix}$, $\mathbf{A}_2 = \mathbf{A}_1 = \mathbf{A}$, $\mathbf{B}_2 = \begin{bmatrix} -U_{in}/L \\ 0 \end{bmatrix}$, $\mathbf{X}=[x_1,\ x_2]=[i_L,\ u_C]$ - state variables vector, i_L - inductor current, u_c - capacitor voltage.

The solution of the system (3) in each segment of structure constancy of the power unit is recorded in the analytical form and a segment-to-segment transition is done using the fitting method.

It can be shown that the system behavior within the k$^{\text{th}}$ cycle period is described by a stroboscopic map:

$$\mathbf{X}_k = \Psi(\mathbf{X}_{k-1}) = e^{\mathbf{A}a}\mathbf{X}_{k-1} + e^{\mathbf{A}(1-z_k)a}\left(e^{\mathbf{A}z_k a} - \mathbf{E}\right)\mathbf{A}^{-1}\mathbf{B}_1 + \left(e^{\mathbf{A}(1-z_k)a} - \mathbf{E}\right)\mathbf{A}^{-1}\mathbf{B}_2, \tag{4}$$

where $\mathbf{X}_{k-1}$ - state variables vector at the beginning of the k^{th} cycle period.

When using SPWM, the sinusoidal control action period contains q cycle periods, where q is called the quantization factor. Suppose that q is an integer. The stroboscopic map for the SPWM system can then be represented as

$$\mathbf{X}_p = \Psi^{(q)}(\mathbf{X}_{p-1}) \equiv \underbrace{\Psi \circ \Psi \circ \Psi \circ \Psi \circ \ldots \circ \Psi}_{q \text{ times}}, \tag{5}$$

where p - map iteration number.

Point of switching z_k in the k^{th} cycle period can be calculated using the switching manifold equation $\xi(\mathbf{X},z_k)=0$ [2]

$$\xi(\mathbf{X}, z_k) = \alpha\left(U_{ref}(k) - \beta u_c(k)\right) - U_{rgm}(2z_k - 1),$$

where $u_c(k)$ - capacitor voltage at the beginning of the k^{th} cycle interval, U_{rgm} - ramp voltage amplitude, $U_{ref}(k)=U_{rm}\sin(\omega_s(k\text{-}1)T)$, U_{rm} - reference signal amplitude, ω_s – control signal frequency.

When using TOC, we will introduce additional control actions u_{1k} and u_{2k}, which are calculated as follows:

$$u_{1k} = K_1\left(x_{1kref} - x_{1clk}\right); u_{2k} = K_2\left(x_{2kref} - x_{2clk}\right),$$

Taking into consideration the above mentioned, the function of the stroboscopic map of the TOC system (3) is as follows:

$$\mathbf{X}_k = \Psi(\mathbf{X}_{k-1}) = e^{\mathbf{A}a}\mathbf{X}_{k-1} + e^{\mathbf{A}(1-(z_k+\Delta z_k))a}\left(e^{\mathbf{A}(z_k+\Delta z_k)a} - \mathbf{E}\right)\mathbf{A}^{-1}\mathbf{B}_1 + \left(e^{\mathbf{A}(1-(z_k+\Delta z_k))a} - \mathbf{E}\right)\mathbf{A}^{-1}\mathbf{B}_2,$$

where Δz_k - duty cycle increment in the k^{th} cycle period.

The mentioned increment can be calculated as (Figure 1)

$$\Delta z_k = \alpha\left(u_{1k} + u_{2k}\right)/U_{pm}.$$

When implementing the discussed control algorithm, the calculation of fixed points arrays of the stroboscopic map (5) is the most important task: $\mathbf{X}_{st1}=[x_{11ref}, x_{12ref}, x_{13ref}, \ldots x_{1qref}]$; $\mathbf{X}_{st2}=[x_{21ref}, x_{22ref}, x_{23ref}, \ldots x_{2qref}]$. The first array is a set of inductor currents (x_{1kref} in Figure 1) over the reference signal period; the second array is a set of capacitor voltages (x_{2kref}). The size of each array is equal to quantization factor q.

To calculate the arrays we need to calculate a fixed map point (5), for which purpose the following equation can be used:

$$\Psi^{(q)}(\mathbf{X}) - \mathbf{X} = 0, \tag{6}$$

where the components of vector $\mathbf{X}^*=[x_{11ref}, x_{21ref}]$ correspond to the first components in arrays $\mathbf{X}_{st1}$ and $\mathbf{X}_{st2}$. The remaining components of arrays $\mathbf{X}_{st1}$ and $\mathbf{X}_{st2}$ can be calculated using the recurrence formula (4).

The transcendental equation (6) can be solved using Newton's method, which requires significant computing power of the microcontroller. To simplify the task in the microcontroller program, we suggest using two neural networks, each of which calculates its own component of the fixed point of the 1-cycle, X^*. Here, neural networks serve as universal approximators. The calculation of the learning sample and neural network teaching are performed using a support computer, for example, in MatLab. Subsequently, the calculated neuron weight factors and network biases can be used in the microcontroller's program. The values of parameters that change over a wide range during the system operation are supplied to the inputs of neural networks created, that is, U_{ref}, U_{in} and R_L, which are sensor-controlled (Figure 1). *RLC* calculates current load resistance based on measured load voltage and load current. *FPC* units calculate and output the components of arrays $\mathbf{X}_{st1}$ and $\mathbf{X}_{st2}$ depending on cycle period *k*.

State variables feedback on the stroboscopic time points in the suggested system (Figure 1) is performed using sample & hold circuits (*SH*1 and *SH*2 in Figure 1). As Fig. 1 shows, the output capacitor *C* voltage and the inductor *L* current are memorized at the beginning of each cycle period when supplying a strobe pulse from master clock *MC*, which operates in synchrony with ramp generator *RG*, to *SH*1 and *SH*2. Using two subtracters (*SB*1 and *SB*2 in Figure 1), the deviation of the current map point position (4) from the preset value is calculated, followed by respective errors scaling using K_1 and K_2 factors. The calculated control actions, u_{1k} and u_{2k} are added to the *MCS* voltage error (U_{err}), causing duty cycle increase Δz_k (expression (5)), which stabilizes the design mode, in each cycle period. When establishing the design 1-cycle in the system, $u_{1k} = u_{2k} = 0$ and $\Delta z_k = 0$.

The suggested control system structure can be implemented using a relatively large range of modern digital signal microcontrollers or low-cost programmable logic integrated circuits.

4. SPWM voltage converter of nonlinear dynamics study

This segment contains the results of mathematical simulation of a TOC control system with a single-phase SPWM bridge inverter.

The following set of parameters were used for the simulation: L=4 mH; C=3.5 μF; R=1 Ohm; $R_н$=45 Ohm; α=6.9; β=0.075; U_{rgm}=10 V; T=0.0001 s, q=10. The results of the mathematical simulation are shown in Fig. 3 in the form of dynamic mode maps, which show special aspects of division of the system parameter space into stability areas of different modes. Here, $A_{i,j}$ indicates the stability area of a dynamic mode (*i* - area specific *m*-cycle; *j* - area number on the dynamic modes map). In particular, area $A_{1,1}$ is the first stability area of the design mode with frequency $f_{sq}=1/T$ (1-cycle). Areas $A_{X,j}$ correspond to the areas of system parameters, where chaotic inverter modes exist [2, 3].

As Figure 3 (a, b) shows, the area of the design 1-cycle area ($A_{1,1}$) of a system with no nonlinear dynamics control is relatively small.

In case of large amplitude of the reference signal, an unwanted 1-cycle ($A_{1,2}$) is implemented in the system with overmodulation in multiple cycle periods. At high input voltages, the area of quasi-periodic oscillations with periodicity areas can be seen (Figure 3a). Figure 3b is a diagram of the RMS value of parasitic harmonics with numbers other than 1 (U_{pg}). Obviously, at high input voltages, the RMS value of parasitic harmonics is large, which causes significant distortion of output voltage sinusoidality.

Fig. 4a shows the dynamic modes map of the TOC-based automatic control system. In such case, the following *AGS* (as shown in Figure 1) parameters were used: $K_1=K_2$=-1.5, $\beta_1=\beta_2$=0.05. The area of

the designed 1-cycle area ($A_{1,1}$) (Figure 4a) is significantly larger compared to the corresponding area in the system with no nonlinear dynamics control (Figure 3a). Also, as Figure 4b shows, the RMS value of parasitic harmonics significantly reduces at large input voltages.

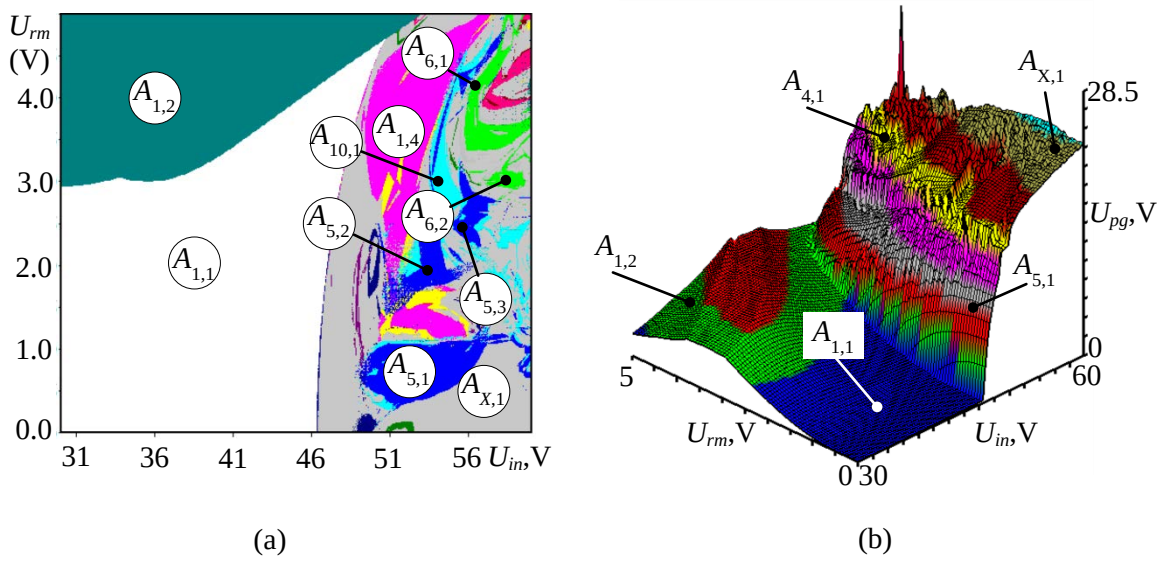

Figure 3. Two-parameter diagrams: (a) dynamic modes map, (b) relative RMS value of parasitic harmonics

As Figure 4a represents, the map still has an area of unwanted 1-cycle $A_{1,2}$ with overmodulation in some cycle periods, making it impossible to eliminate such mode.

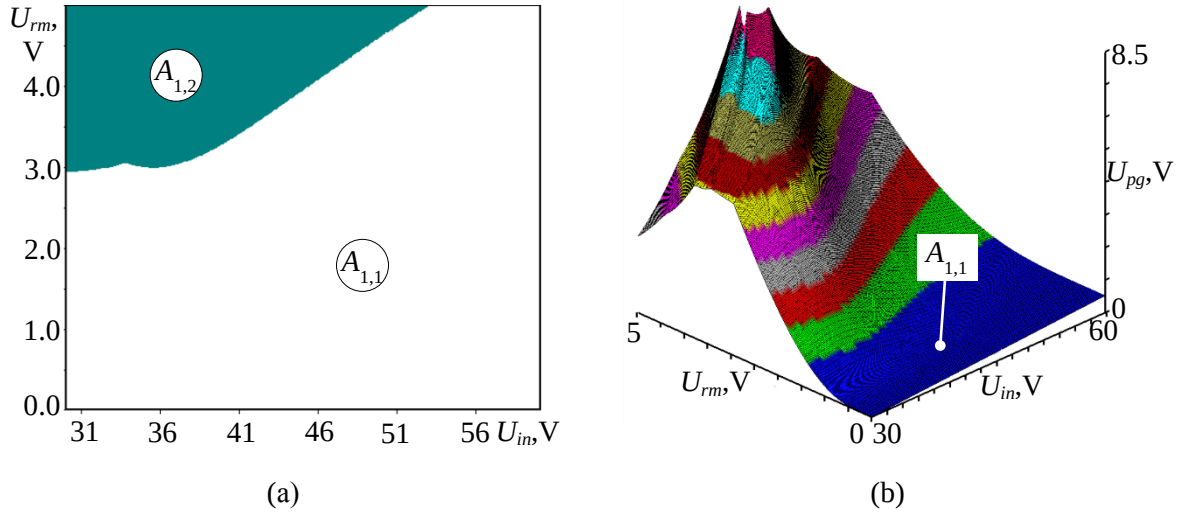

Figure 4. Two-parameter diagrams: (a) dynamic modes map, (b) relative RMS value of parasitic harmonics of the output voltage

Figure 5 is a waveform showing the transition from the unwanted dynamic mode to the design 1-cycle using the discussed control algorithm. The control algorithm starts to operate at t=0.15 s. As the Figure shows, the output voltage oscillation amplitude in the design mode is significantly lower than in the unwanted mode, which indicates the hazard of the latter.

Thus, it can be concluded that the use of TOC has significantly improved the nonlinear dynamic properties of the system, wherein the proportional controller gain remained unchanged, allowing, in this case, keeping a predetermined static error.

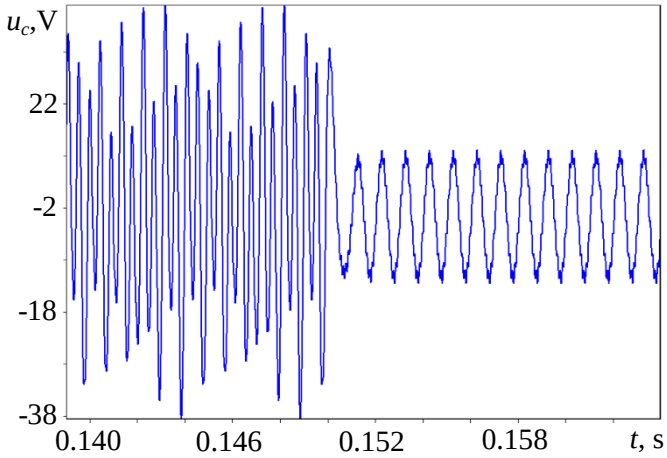

Figure 5. Waveforms at U_{in} = 55 V and U_{rm} = 1 V

5. Conclusion

The target-oriented control of nonlinear dynamics of the SPWM automatic control system has been discussed. The method has been applied to control the SPWM system for the first time. The results show that when using the selected parameters, the TOC system is able to significantly extend the range of the design dynamic mode without having to adapt the method parameters. This control algorithm requires significant computational resources of the microcontroller and can be used for controlling the nonlinear dynamics of inverters with other types of SPWM, with a minor modification stroboscopic map.

References

[1] Ismail B, Mieee S T, Mohd A R, Saad M I and Hadzer C M 2006 *First International Power and Energy. Conference Pecon 2006 November 28-29, 2006, Putrajaya, and Malasia* 437–440
[2] Zhusubaliyev Zh T, Mosekilde E, Andriyanov A I and Shein V V 2014 *Physica D: Nonlinear Phenomena* **268** 14-24
[3] Ming Li,·Dong Dai and Xikui Ma 2008 *Circuits Syst Signal Process* **27** 811–831
[4] Ott E, Grebogi C., Yourke G. 1990 *Phys. Rev. Lett* **64** 1796–1199
[5] Pyragas K 1992 *Phys. Rev. Lett.* A **170** 421–428
[6] Batlle C, Fossas E and Olivar G 1999 *International Journal of Circuit Theory and Applications* **27** 617–631
[7] Zhou Yufei, Tse Chi K, Qiu Shui-Sheng and Lau Francis C M 2003 *International Journal of Bifurcation and Chaos* **13** 3459–3471
[8] Wei Jiang, Fang Yuan and Wen-long Hu 2011 *Applied Mechanics and Materials* **39** 1–6
[9] Naihong Hu, Yufei Zhou and Junning Chen 2012 *Journal of Information & Computational Science* 9 **2** 497–504
[10] Dattani J, Blake J C H and Hilker F M 2011 *Phys. Lett.* A **375** 3986–3992
[11] Andriyanov A I and Krasnov N I 2013 *Izvestiya vysshikh uchebnykh zavedeniy. Priborostroenie* **56** 33–38
[12] Haykin S 2009 *Neural Networks and Learning Machines*. (New Jersey: Prentice Hall)